Adhesion Structures of Amniotic Membranes Integrated into Human Corneas

Miklós D. Resch,[1] *Ursula Schlötzer-Schrehardt,*[2] *Carmen Hofmann-Rummelt,*[2] *Renate Sauer,*[2] *Claus Cursiefen,*[2] *Friedrich E. Kruse,*[2] *Matthias W. Beckmann,*[3] *and Berthold Seitz*[2]

Purpose. The aim of this study was to investigate the structural relationship between integrated amniotic membrane (AM) and corneal tissues in various integration patterns, focusing on adhesion structures along the interface.

Methods. Fourteen eyes of 14 patients (age, 65.8 ± 13.5 years) underwent penetrating keratoplasty (PKP) 19.3 ± 20.7 weeks after cryopreserved human AM transplantation (AMT). The corneal buttons (after PKP) and the corresponding original AM (before AMT) were examined with the use of transmission electron microscopy (TEM) and immunohistochemistry for integrin β4, type VII collagen, and laminin. Main outcome measures included thickness of the corneal epithelium and AM, density of the epithelial desmosomes and hemidesmosomes, continuity, and thickness of the epithelial basement membrane.

Results. Integrated AM was found by slit lamp in only 2 of 14 patients, but histology and TEM revealed AM integration in 11 of 14 patients up to 77 weeks after AMT. No amniotic epithelial cell was detected in any cornea with integrated AM stroma. Three basic patterns of integration could be described: subepithelial, intraepithelial, and intrastromal. Hemidesmosomes anchored the corneal epithelial cells to the AM at a density up to 165.3 ± 22.9 per 100 μm cell membrane length. Discontinuous basement membrane segments 17.2 ± 4.9 nm thick could be detected. Desmosomes among recovered corneal epithelial cells were found at a density of 21.2 ± 5.3 per 10 μm cell membrane length.

Conclusions. The AM stroma can integrate into the host corneal tissue. Integration is associated with the formation of adhesion structures such as hemidesmosomes and desmosomes, which provide anchoring and stability of the regenerating corneal epithelium. The presence of integrated AM and adhesion structures with host corneal tissue supports the clinical experience obtained with AMT in ocular surface disease. (*Invest Ophthalmol Vis Sci.* 2006;47:1853–1861) DOI: 10.1167/iovs.05-0983

From the [1]1st Department of Ophthalmology, Semmelweis University, Budapest, Hungary; and the Departments of [2]Ophthalmology and [3]Gynecology and Obstetrics, University of Erlangen-Nürnberg, Erlangen, Germany.

Supported in part by Eötvös Scholarship No. 63/2004 of the Hungarian Ministry of Education.

Submitted for publication July 27, 2005; revised December 20, 2005, and January 18, 2006; accepted March 13, 2006.

Disclosure: **M.D. Resch**, None; **U. Schlötzer-Schrehardt**, None; **C. Hofmann-Rummelt**, None; **R. Sauer**, None; **C. Cursiefen**, None; **F.E. Kruse**, None; **M.W. Beckmann**, None; **B. Seitz**, None

The publication costs of this article were defrayed in part by page charge payment. This article must therefore be marked "*advertisement*" in accordance with 18 U.S.C. §1734 solely to indicate this fact.

Corresponding author: Miklós Resch, 1st Department of Ophthalmology, Semmelweis University, Tömö utca 25–29, 1083, Budapest, Hungary; remi@szem1.sote.hu.

The amniotic membrane (AM) is the innermost layer of the fetal membrane, and it is used as surgical material in reconstructive ocular surface surgery.[1–3] AM consists of a stromal layer, a basement membrane, and a monolayer of cuboid epithelial cells.[4] The stroma can be further divided into an acellular compact layer (lamina densa), a fibroblast layer (lamina fibroreticularis), and a spongy layer (lamina propria).[5] None of the AM layers contain blood vessels. The surgical application of AM has been used in a variety of ocular surface disorders[6–8] because of its availability and convenience and its anti-inflammatory,[9–11] antifibroblastic,[12] antimicrobial,[13] and antiangiogenic[14] properties. AM has also been used as a carrier substrate for ex vivo expansion of limbal stem cells[15–18] and keratocytes.[19]

Other than favorable clinical results after AM transplantation (AMT),[20–22] few studies report histologic findings in human corneas after AMT.[23–25] Therefore, the exact time course and patterns of corneal wound healing and integration of AM into the cornea are still not clearly established. Knowledge of the connection between AM and cornea could add information to our clinical experience and thereby improve the application techniques of AMT. The aim of this study was to investigate the histologic and ultrastructural aspects of the structural relationship between the AM and corneal tissues in various patterns of AM integration, focusing on adhesion structures involved in cell–cell and cell–matrix interactions along the corneal epithelium–AM interface.

Materials and Methods

Patients

Between July 1999 and October 2004, 24 eyes of 24 patients underwent penetrating keratoplasty (PKP) after AMT out of a total of 320 AMTs (Department of Ophthalmology, University of Erlangen-Nürnberg, Erlangen, Germany). Of these 24 patients, 14 (10 men, 4 women; mean age, 65.8 ± 13.5 years; range, 46–89 years) were included in the study. The patients had diverse ocular surface abnormalities that indicated AMT. Clinical and demographic data are summarized in Table 1. All patients had persistent epithelial defects and stromal thinning before AMT as a result of infectious or autoimmune processes. Lesion sizes were measured using the Haag-Streit slit lamp. Mean measurements of the ulcers were: vertical diameter, 2.5 ± 0.7 mm (range, 2–4 mm); horizontal diameter, 4.1 ± 1.6 mm (range, 2–7 mm); depth, 55.8% ± 31.3% (range, 10%–90%) stromal thickness. Stromal vascularization occurred in four eyes. PKP was indicated as an elective surgery in seven eyes 27.4 ± 25.6 weeks (range, 6–77 weeks) after AMT to remove the corneal opacity causing visual impairment. In the other seven eyes, emergency PKP was necessary because of recent or impending corneal perforation 11.2 ± 10.8 weeks (range, 0.3–26 weeks) after AMT. The localization of AM or integration into the cornea was assessed by standard slit lamp examination performed before PKP (Fig. 1). Fluorescein dye was used to determine epithelial defects on the AM surface. Biomicroscopic evidence of AM integration into the cornea was defined as a smooth epithelial surface and an absence of fluorescein dye on the surface of the AM.

Table 1. Clinical and Demographic Data of Patients

Patient						Ulcer before AMT				
Patient	Initials	Age (y)	Gender	Eye	Diagnosis	Horizontal Diameter (mm)	Vertical Diameter (mm)	Depth (% of stroma)	Hypopyon (mm)	Vascularization (quadrants)
1	B.H.	76	M	OD	Persistent epithelial defect, bullous keratopathy, cornea guttata	3	2	20	0	0
2	H.K.	47	F	OD	HSV ulcerative keratitis + bacterial superinfection	5	3	90	1	4
3	M.H.	75	M	OS	HSV ulcerative keratitis	2	2	40	0	0
4	P.M.	46	M	OD	HSV ulcerative keratitis + bacterial superinfection	3	3	40	1	2
5	S.M.	62	F	OD	Infectious keratitis of unknown origin	4	3	20	2	0
6	W.J.	75	M	OD	Bullous keratopathy + bacterial superinfection	7	4	30	0	0
7	K.J.	43	M	OS	Chemical burn	10	9	10	0	0
8	B.W.	73	M	OS	Bacterial ulcer	3	2	90	3	0
9	B.A.	63	M	OS	HSV ulcerative keratitis	3	2	40	0	4
10	D.B.	66	M	OS	Rheumatic marginal ulcer	4	2	50	0	0
11	D.R.	64	F	OD	Rheumatic ulcer, descemetocele	5	3	90	0	0
12	D.K.	89	F	OD	Pseudophakic bullous keratopathy, rheuma, cornea guttata	6	3	MD	0	0
13	P.A.	80	M	OD	HSV ulcerative keratitis	2	2	90	0	0
14	R.E.	62	M	OS	Metaherpetic keratitis	6	2	70	0	3

g, graft; p, patch; MD, missing data; Single, multiple interrupted single sutures; Cont, double running continous suture.

Surgical Technique

Amniotic Membrane Transplantation. AMs were obtained at elective cesarean section, prepared under sterile conditions, and cryopreserved at −80°C, as described by Tseng and Kruse.[3,22] The medium used for preservation contained 250 mL sterile glycerine filtered to 0.45 μm, 250 mL Dulbecco modified Eagle medium, 50,000 U penicillin, 50 mg streptomycin, and 1.25 μg amphotericin B. Different techniques of AMT (graft, patch, and sandwich) have been described by Kruse,[20] Seitz,[25,26] Prabhasawat,[27] Letko,[28] and others. In all cases, AM was transplanted with the epithelium and the basement membrane side up. When repeat AMT (four eyes) was performed, AM parts that persisted from the previous AMT were completely removed. In these cases, time interval to PKP was counted from the last AMT. At the completion of AMT, all patients received a bandage contact lens that was left in place for 4 weeks unless keratoplasty was performed earlier. Choice of postoperative medication depended on the ocular abnormality, but all patients received preservative-free antibiotic eye drops 3 times a day, artificial tears 5 to 10 times a day, and preservative-free cycloplegics 2 times a day. Topical corticosteroid (prednisolone acetate) therapy was given not more than 2 to 3 times a day. All patients with herpetic infection were treated topically with trifluorothymidine drops 4 times a day and with 5 × 400 mg systemic acyclovir for 4 weeks and then with 2 × 400 mg acyclovir for at least 6 months after surgery.

Penetrating Keratoplasty. PKP was performed with mechanical trephination in 13 eyes to preserve as much tissue as possible and with elliptical 193 nm excimer laser nonmechanical trephination[29,30] in one eye. Size and technique of trephination were adapted to the condition of the recipient eye[31]; graft diameters are shown in Table 1. Nylon sutures (10–0) were applied as multiple interrupted sutures in nine eyes or as double-running sutures in five eyes. Postoperative therapy was similar to that after AMT. As soon as the epithelium closed, prednisolone acetate eyedrops were administered for the next 6 months.

Light and Electron Microscopy

After PKP, the excised corneal buttons were fixed in 10% formaldehyde, bisected taking care of the AM location, and processed for routine light microscopy, immunohistochemistry, and transmission electron microscopy (TEM). The TEM halves were postfixed in 2% buffered osmium tetroxide, dehydrated in graded alcohol concentrations, and embedded in epoxy resin (Epon 812; Fluka, Buchs, Germany) according to standard protocols. After AMT, the remaining

			Status before PKP		Penetrating Keratoplasty			
AMT1	AMT2 after AMT1 (wk)	AMT2	PKP after AMT (wk)	Cornea	Diameter of Corneal Trephination (recipient mm/donor mm)	Suture	Type	PKP Combined with
1g	—	—	12	Retracted AM, erosion	7.5/7.6	Single	Elective	—
5g + 1p	26	2g	17	Retracted AM	7.0/7.25	Single	Elective	—
1g + 1p	—	—	21	Retracted AM	7.0/7.3	Cont	Elective	Cataract extraction + IOL implantation
3g + 1p	10	1g + 1p	12	Corneal scar	7.0/7.5	Single	Elective	Cataract extraction + IOL implantation
3g	—	—	47	Integrated AM	7.5/7.75	Cont	Elective	—
2g + 1p	—	—	6	Integrated AM	7.0/7.3	Cont	Elective	—
1g + 1p	—	—	77	Retracted graft, vascularization	MD	Cont	Elective	—
2g + 1p	—	—	2	Retracted AM, erosion	6.2/6.7	Single	Emergency	Simultaneous AM patch
3g + 1p	9	4g + 1p	25	Corneal ulcer	7.0/7.25	Cont	Emergency	—
1g	—	—	26	Perforated	7.0/7.5	Single	Emergency	Horse shoe-shaped sclerokeratoplasty
4g + 1p	—	—	3	Perforated under AM	7.5/8.0	Single	Emergency	—
1g	—	—	0.3	Degraded AM	7.5/7.8	Single	Emergency	—
3g	—	—	14	Focal perforation	7.0/7.25	Single	Emergency	—
4g	52	2g + 1p	8	Corneal ulcer	7.0/7.5	Single	Emergency	—

portions of the original AM not used for transplantation were processed identically. Three healthy donor corneas obtained from the Cornea Bank of Erlangen served as controls. Semithin sections (1 μm) were stained with toluidine blue to determine the pattern of integrated AM by light microscopy. Integration of AM into the cornea was defined as the intracorneal presence of epithelial or stromal components of the AM. Monoclonal antibodies raised against human integrin β4 (diluted 1:50; Chemicon, Temecula, CA) and human collagen type VII (diluted 1:50; Chemicon) were used to identify hemidesmosomes and anchoring fibrils, respectively. Immunolabeling experiments were performed on 5-μm–thick paraffin-embedded sections using the peroxidase-labeled streptavidin-biotin method (LSAB Plus-kit; DAKO, Glostrup, Denmark) according to the manufacturer's instructions. 3-Amino 9-ethyl carbazol (AEC) was used as a chromogenic substrate, and Mayer hemalum was used as a counterstain. In negative control experiments, the primary antibody was replaced by PBS or equimolar concentrations of an irrelevant primary antibody. Before immunolabeling, antigen retrieval was achieved by heating the slides immersed in Tris-EDTA buffer, pH 9.1, in a commercial microwave oven at 160 W for 15 minutes. Ultrathin sections were cut and stained with uranyl acetate–lead citrate and examined with a transmission electron microscope (EM 906E; Zeiss, Oberkochen, Germany).

Main Outcome Measures of Electron Microscopic Analysis

Patterns of AM Integration into the Cornea. At low magnifications (×600 to ×2500), the integration patterns of AM were evaluated, and the number of corneal epithelial cell layers, the thickness of corneal epithelium, and the thickness of AM layers were measured.

Cell–Matrix and Cell–Cell Adhesion Structures. At higher magnifications (×6000 to ×46,500), the density of hemidesmosomes between epithelial cells and basement membrane in the corneal buttons and in the original AM were determined. Hemidesmosomes were counted along the basal cell membrane of 10 randomly selected basal corneal epithelial cells, and density was indicated as number of hemidesmosomes per 100 μm cell membrane length. The presence and continuity of the basement membrane were determined and indicated in the percentage of cell length. The thickness of the basement membrane was measured. The density of desmosomes in 10 randomly selected corneal epithelial cells was indicated as the number of desmosomes per 10 μm cell membrane length. Each measurement was performed in five randomly selected regions of sections.

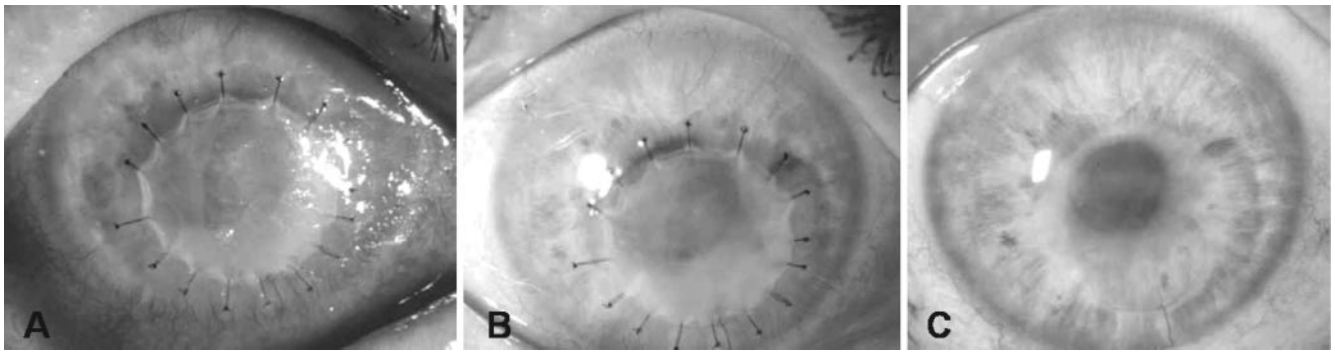

FIGURE 1. Slit lamp observation of the AM integration process in the cornea of patient 5. Therapy-resistant central keratitis of unknown cause was treated with triple-layer graft AMT. (**A**) One week after AMT, the uppermost layer of the AM graft was still in place, but it had thinned and was not covered by corneal epithelium. (**B**) Twelve weeks after AMT, the surface of the cornea was regular, and the AM was covered by corneal epithelium. (**C**) Forty-seven weeks after AMT (before penetrating keratoplasty was performed), sutures had been removed, and the AM grafts were integrated and appeared more transparent.

Statistical Analysis

Statistical analysis was performed (SPSS 10.0 for Windows; SPSS Inc., Chicago, IL). Data are presented as mean ± SD. Statistical evaluation of significant differences between patients or tissues was carried out with the Mann-Whitney *U* test. Corneal epithelial cell and adhesion structure parameters were compared with control corneas. The thickness of the AM integrated into the cornea was compared with that of the original (not transplanted) AMs. $P < 0.05$ was considered statistically significant.

RESULTS

Original cryopreserved AM was covered by a monolayer of cuboid amniotic epithelium (Fig. 2A). The cells showed signs of degeneration, such as vacuolar translucent cytoplasm, cytoplasmic vesicles, and multivesicular bodies (Fig. 2B). Neighboring amniotic epithelial cells were interconnected by desmosomes and complex membrane interdigitations. Their basal surfaces formed podocyte-like processes attached to the basement membrane by hemidesmosomes at a density of 214.2 ± 32.8 (range, 143–221). Under the AM epithelium, a 182.1 ± 13.4 (158–197)-nm thick continuous basement membrane was observed after the undulations of the epithelial basal cell surface. The thickness of the underlying AM stroma varied considerably from 12.1 μm to 66.4 μm (43.3 ± 34.5 μm) and contained loosely, irregularly arranged collagen fibers and a few degenerative-appearing fibrocytes (palisade cells) in the deeper layers.

The integration of AM into corneal tissue was clearly detected by slit lamp examination in only 2 of 14 patients. In 7 of 14 patients, a retracted or residual AM was found, whereas 5 of 14 patients showed no biomicroscopic evidence of AM presence. However, histologic examination revealed AM integration in 11 of 14 patients. Integrated AM stroma was found from 2 to 77 weeks after AMT. No AM epithelial cells were identified in any of the corneas examined. The integrated AM stroma contained some fibrocytes, but at a lower density, than that of the normal corneal stroma.

The AM stroma was integrated into the corneal tissue in three basic patterns—subepithelial integration, intraepithelial integration, and intrastromal integration—resulting in different structural interfaces between AM and corneal tissue. Some corneal specimens revealed more than one pattern in different areas.

Pattern 1: Subepithelial Integration of AM (Corneal Epithelium Covering Top of AM Stroma)

In most (10/14) of the patients (Table 2), one or more layers of AM stroma were detected subepithelially and were directly overgrown by corneal epithelium. Bowman's layer was either lacking (7/10 patients) or present (3/10 patients) under the AM stroma. The thickness of the integrated AM stromal layers was markedly, though not statistically significantly, reduced compared with the control AM. The number of corneal epithelial layers and the thickness of the epithelium showed variability (Fig. 3A). Desmosome density among corneal epithelial cells

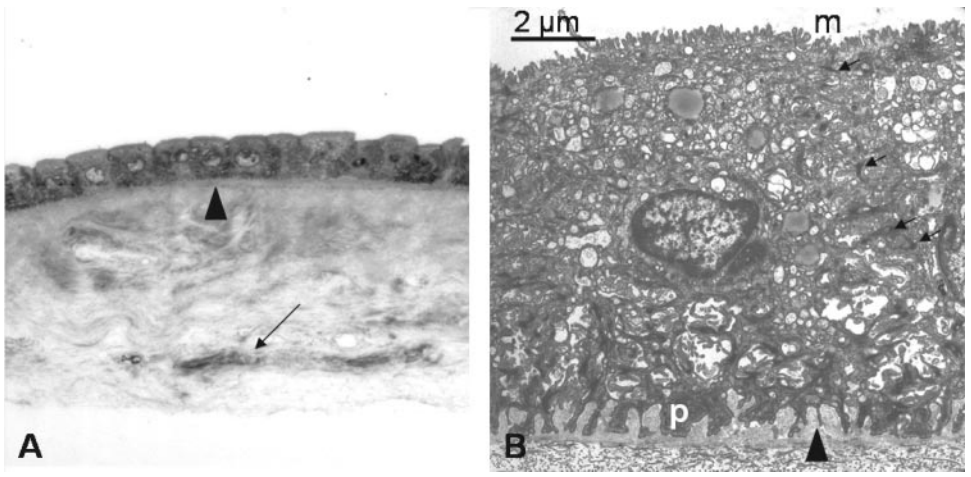

FIGURE 2. Original cryopreserved AM. (**A**) Light microscopy semithin section (toluidine blue; original magnification, ×400) of the AM. A monolayer of cuboid epithelial cells covered the thick basement membrane (*arrowhead*). The stroma contained few degenerative fibrocytes (*arrow*) and irregularly arranged collagen fibers. (**B**) Transmission electron micrograph of AM epithelium. Note the microvilli (m) on the apical surface, the membrane interdigitations between adjacent epithelial cells (*arrows*), and the podocyte-like (p) cell processes attaching to the basement membrane (*arrowhead*). Cryopreservation caused degenerative alterations in the cytoplasm.

TABLE 2. Parameters of Corneal Epithelial Cells, AM Stroma, and Cell Matrix Adhesion Structures

	Patient No. with Respective Patterns	Corneal Epithelium		AM Thickness (μm)	Hemidesmosome Density/100 μm	Basement Membrane		Desmosome Density/10 μm
		No. Layers	Thickness (μm)			% of Cell Length	Thickness (nm)	
Control corneas	—	6.1 ± 1.4 (5; 7)	51.3 ± 10.6 (39.1; 63.1)	NA	187.5 ± 22.4 (154; 211)	98.2 ± 3.1 (81; 100)	18.2 ± 4.1 (14; 20)	22.1 ± 4.8 (16; 26)
Control AM	1–14	NA	NA	43.3 ± 34.5 (12.1; 66.4)	214.2 ± 32.8 (143; 221)	100	182.1 ± 13.4 (158; 197)	25.6 ± 2.6 (21; 30)
Subepithelial integration	1–9, 13, 14	6.2 ± 2.3 (4; 8)	52.3 ± 14.3 (40.1; 69.2)	29.8 ± 5.4 (22.1; 46.1)	165.3 ± 22.9 (142; 189)	28.4 ± 10.2* (21; 41)	14.5 ± 5.6† (9; 20)	21.2 ± 5.3 (15;26)
Intraepithelial integration	1, 2, 8, 9	1.2 ± 0.4* (1; 2)	18.3 ± 3.6* (13.4; 22.1)	34.5 ± 20.3 (15.2; 56.3)	54.2 ± 21.8* (31; 67)	Fragments	NA	19.8 ± 5.3 (18; 24)
Intrastromal integration	4, 6, 9, 13	8.4 ± 3.1* (5; 11)	61.4 ± 23.1 (45.3; 85.3)	6.9 ± 7.8† (0; 16.7)	178.4 ± 20.3 (153; 195)	54.3 ± 18.6* (41; 76)	15.6 ± 3.4† (10; 19)	16.2 ± 4.3* (9; 18)

Values are given as mean ± SD (min; max). Each measurement was performed in five randomly selected regions.
* Comparison with Mann-Whitney *U* test ($P < 0.05$) to the control cornea.
† Compared with the original AM with Mann-Whitney *U* test ($P < 0.05$).

was not different from that of control corneas (Table 2). Basal corneal epithelial cells were columnar (Fig. 3B). Well-developed hemidesmosomes anchored the basal corneal epithelial cells to the underlying AM stroma at a slightly lower density than the control corneas (Fig. 3C). Only short segments of basement membrane were present along less than one third of the cell membrane. The thickness of the basement membrane segments was slightly reduced but was not significantly different from that of control corneas. Within this pattern, some subtypes could be distinguished.

In patients 1, 6, and 7 (Fig. 3D), Bowman's layer was intact and corneal epithelium partly covered the AM and Bowman's layer. The corneal epithelium covering AM displayed fewer layers and reduced thickness than did areas covering the Bowman's layer, thus forming a smooth surface contour (Fig. 3D, 3E). Occasionally, small patches of residual AM stroma were detected between the corneal epithelium and Bowman's layer. Small bundles of anchoring fibers could be identified by TEM (Fig. 3F). In patient 7, the corneal epithelium was thought, because of histology, to be anchored to the Bowman's layer, but TEM showed cross-sectioning of collagen fibrils and electron-dense vacuoli between Bowman's layer and the corneal epithelium.

The integrated AM revealed a highly irregular structure and signs of degeneration in specimens 2, 3, 4, 5, 9 (Fig. 3G), and 13, including areas of condensed, degenerative, or dissolved AM stroma (Fig. 3H, 3I). In these patients, the morphology of basal corneal epithelial cells and the density of desmosomes and hemidesmosomes were similar to those in patients with regular AM stroma.

Pattern 2: Intraepithelial Integration of AM (Corneal Epithelium Sandwiching AM Stroma)

In patients 1 and 9, Bowman's layer was intact and the corneal epithelium grew over the AM, but light microscopy revealed one or more layers of corneal epithelial cells between AM and Bowman's layer (Fig. 4A). The corneal epithelial layers covering the top of AM were not different from those in pattern 1 (corneal epithelium covering top of AM stroma) concerning cellular ultrastructure and cell–cell adhesion structures. Corneal epithelial cells under the AM disclosed a regular ultrastructure and close contact with the AM and with the Bowman's layer (Fig. 4B). Hemidesmosomes and basement membrane were observed along the apical and the basal cell surfaces of the corneal epithelial cells under AM (Fig. 4C). In patients 2 and 8, Bowman's layer was missing, but the AM stroma was covered by corneal epithelium on the superficial and basal surfaces.

Pattern 3: Intrastromal Integration of AM (Corneal Epithelium Covering AM Stroma Integrated into Corneal Stroma)

In regions of corneas 4, 6, 9, and 13, the corneal epithelium had overgrown the anterior part of the stroma resembling either the corneal or the amniotic stroma. The origin of the stromal structure could not be determined exactly by light microscopy. In addition, the irregular stromal structure could be interpreted as corneal scar tissue or as intrastromal integration of the AM stroma. The corneal stromal surface and the thickness and number of corneal epithelial layers appeared highly irregular by light microscopy (Fig. 5A). Basal corneal epithelial cells had a degenerative appearance (Fig. 5B), as indicated by electron lucent cytoplasm, pale nuclei, and abundant intracellular vacuoles. Desmosomes among degenerative basal corneal epithelial cells were present at a statistically lower density than in controls (Table 2). Poorly developed hemidesmosomes (Fig. 5C) were observed, but their density was not different from that of the control corneas. Only patches of basement membrane were observed. The corneal epithelium was adapted to the morphology of the underlying stromal lesion (Fig. 5D). Deep stromal layers contained regularly organized lamellae (Fig. 5E). In the interface of corneal epithelium and corneal stroma, no evidence of persisting AM structure was observed, but electron-dense vacuoles could be interpreted as remnants of AM (Fig. 5F).

In patient 11, the AM stroma covered the corneal stroma but was not covered by epithelium. This pattern was defined as superficial localization of AM. No cell–cell or cell–matrix adhesion structures could be detected. In the interface of AM stroma and corneal stroma, no particular structure was found.

Immunohistochemistry revealed a linear immunoreactivity for integrin $\beta 4$ along the basal aspect of the CE overgrowing the amniotic stroma, indicating the presence of hemidesmosomes (Fig. 6A, 6B, arrows). Collagen type VII was detected as a linear fuzzy immunoreaction along the basal aspect of the CE overgrowing AM, providing evidence for the presence of anchoring fibrils (Fig. 6C). Antibody reaction was abolished completely when the primary antibody was omitted (Fig. 6D).

DISCUSSION

Evidence of AM integration is an important milestone in the understanding of the structural relationship between amniotic membrane and cornea. The differences in detecting AM in cornea by biomicroscopic examination, light microscopy, and TEM indicated that the AM is integrated in the cornea more

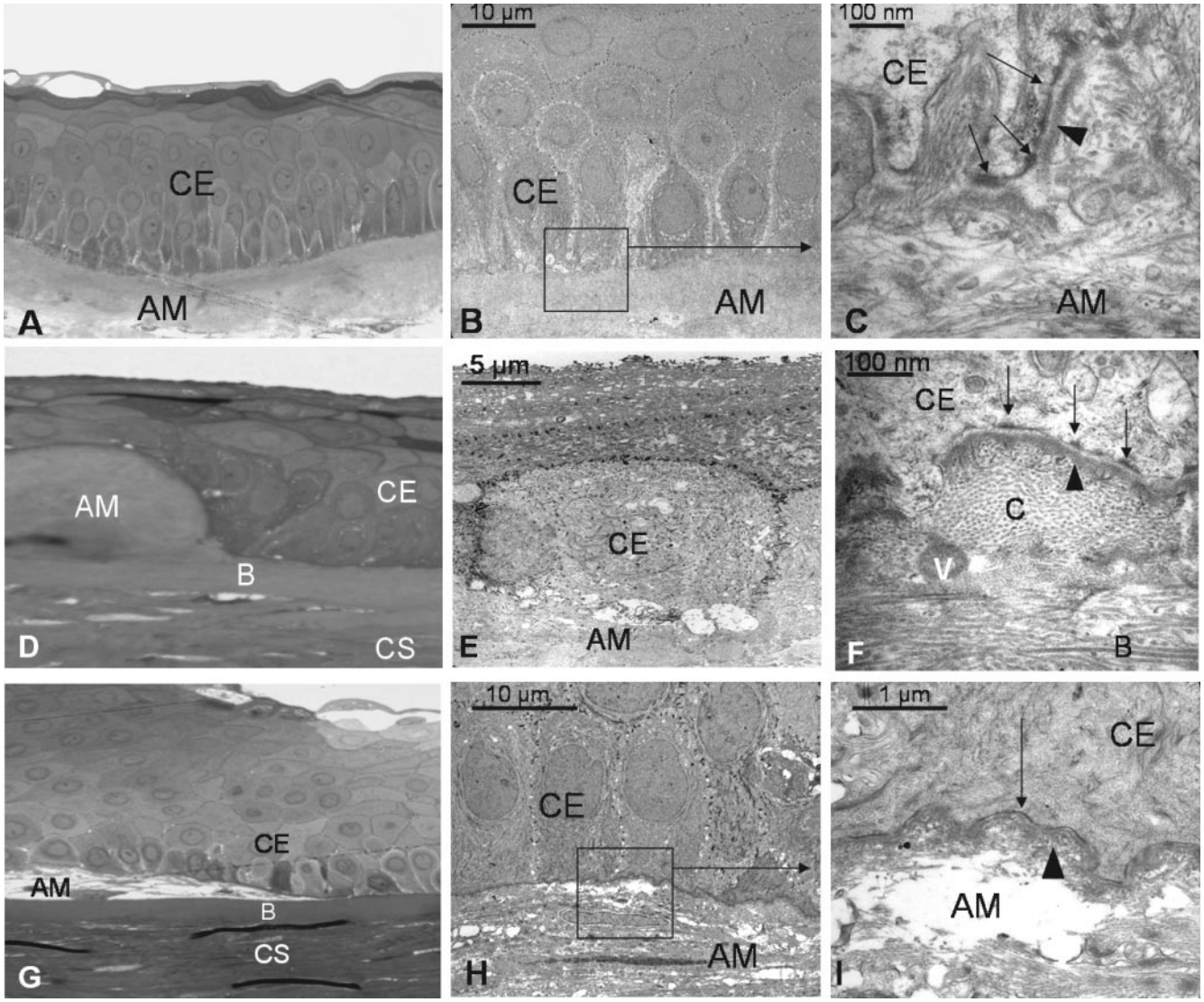

FIGURE 3. Subepithelial integration of AM. Corneal epithelium (CE) covering top of AM (pattern 1). (**A**) Semithin section of the anterior cornea 6 weeks after AMT (patient 6; original magnification, ×100). Bowman's layer is absent. AM stroma without AM epithelium is overgrown by multilayered CE. (**B**) Transmission electron micrograph of the CE covering the AM stroma. Basal CE cells are regular and columnar (patient 6). (**C**) Detail showing cell–matrix adhesion structures of CE on AM stroma. Hemidesmosomes (*arrows*), discontinuous segments of basement membrane (*arrowhead*), and irregularly arranged collagen fibrils of AM stroma (patient 6). (**D**) Semithin microphotograph (original magnification, ×400) of the anterior cornea 77 weeks after AMT (patient 7). On the *left* side the AM was preserved, and on the *right* side it was microscopically absorbed. (**E**) Ultrastructure of a cuboid basal corneal epithelial cell on AM (patient 7). (**F**) Hemidesmosomes (*arrows*) anchored the basal corneal epithelial cells to the underlying basement membrane (*arrowhead*) and remnants of AM overlying Bowman's layer (B). Cross-section of collagen fibrils (C) with smaller diameter than in Bowman's layer and with electron-dense vacuoli (V) (patient 7). (**G**) Semithin section from patient 9 (25 weeks after AMT; original magnification, ×400). Thick, multilayered epithelium attached partly to Bowman's layer and partly to the irregular AM. Structure of the irregular AM stroma was loose, in contrast to the corneal stroma and the original AM stroma. (**H**) Transmission electron micrograph of the basal CE covering the irregular AM (patient 9). Structure of the AM was disorganized. Basal CE cells were regular and columnar. (**I**) Detailed enlargement of *inset* in **H** showing hemidesmosomes (*arrows*) and segments of the basement membrane (*arrowhead*) over irregular, loose AM stromal tissue.

often than was observed with the use of slit lamp examination. In agreement with the findings of Connon et al.[32] in their study of rabbits, the persistence of AM stroma could be identified in most patients; however, no AM epithelium was present in the cornea after AMT. Portions of cryopreserved AM not used for transplantation were covered with AM epithelium in all patients but showed ultrastructural signs of degeneration by TEM. This finding supports the theory presented by Kruse et al.,[22] based on vital stainings, that no viable AM epithelial cells are present after the cryopreservation of AM. In our previous study, we identified persisting AM epithelial cells in corneas earlier than 6 weeks after AMT,[25] but none of the corneas in the present study contained AM epithelial cells.

Gris[22] reported two cases after monolayer AMT. AM remnants were found by light microscopy 3 months after AMT but not 7 months after AMT. After simultaneous transplantation of an AM patch and limbal stem cells, Stoiber et al.[23] investigated four eyes with complete limbal stem cell deficiency caused by severe chemical burn. They could not detect AM with the use of slit lamp examination 5 to 13 months after AMT. However, remnants of AM were detectable in three of the four eyes by histologic examination. In these histologic studies, the adhesion structures were not investigated in detail. In contrast, Tosi[33] examined five corneas 2 to 20 months after AMT and did not find any remnants of AM by histologic examination. In our study, the presence of AM in the cornea was evident by light

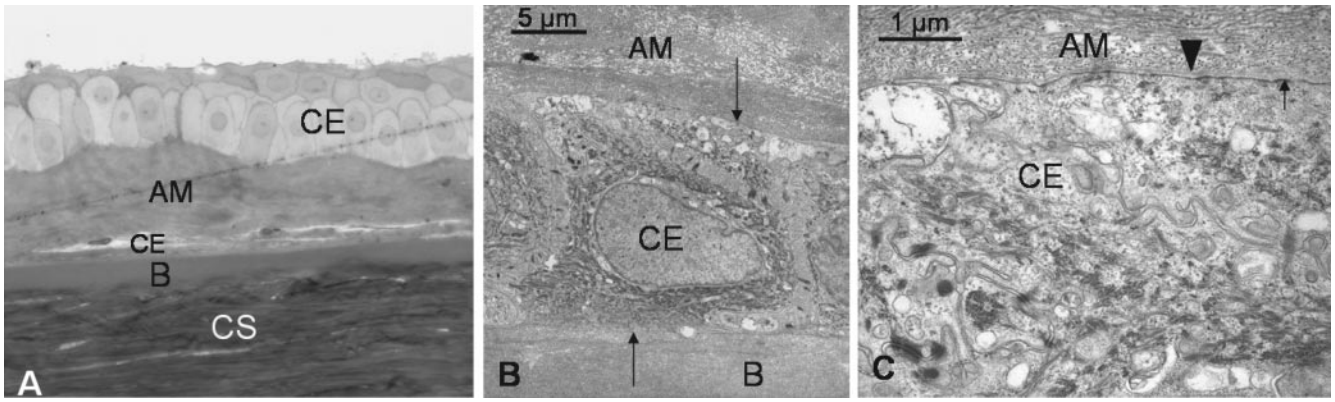

FIGURE 4. Intraepithelial integration of AM. Corneal epithelium (CE) sandwiching AM (pattern 2, patient 1; 12 weeks after AMT). (**A**) Semithin microphotograph (original magnification, ×400). Note the integrated AM and the corneal epithelial cells between AM and Bowman's layer (B). (**B**) Transmission electron micrograph of a CE cell between AM and Bowman's layer (B). Close contact (*arrows*) was found on both sides of the cell. (**C**) Hemidesmosome (*arrow*) between CE and the nonepithelial side of AM stroma. Note the corneal epithelial basement membrane (*arrowhead*; TEM).

microscopy and was confirmed by TEM. A possible explanation for the results of Tosi[33] is the lack of electron microscopic examination and the single-layer AM transplantation (presumably as a patch).

We hypothesized that the density of hemidesmosomes and desmosomes in corneal epithelium in corneas after AMT could be a morphologic correlate for the adhesion of corneal epithelial cells and the stability of corneal epithelial wound healing. Madigan et al.[34] found a correlation between reduced hemidesmosome density and reduced corneal epithelial adhesion in cats. Kyung et al. (*IOVS* 2003;44:ARVO E-Abstract 1362) reported in a rabbit model the primitive structure and the lower

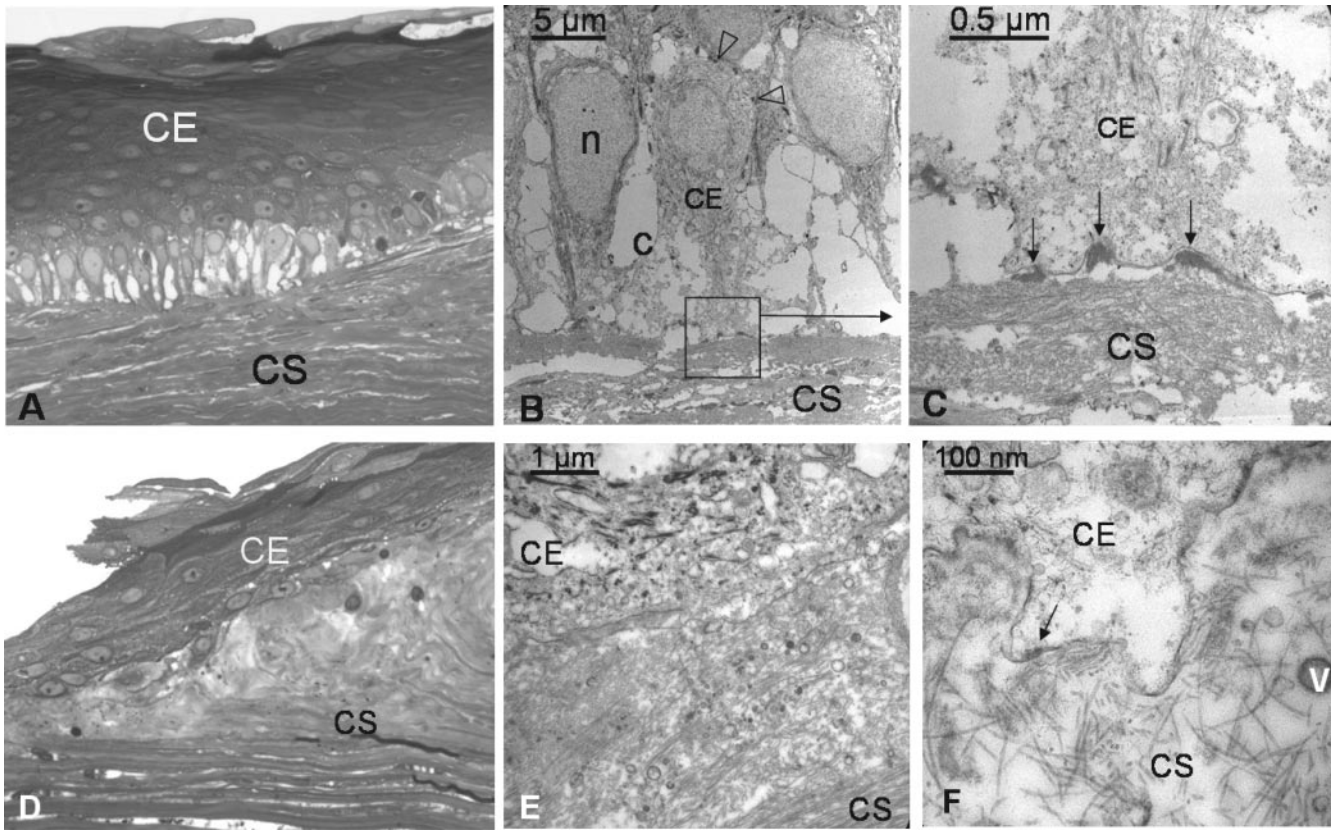

FIGURE 5. Intrastromal integration of AM. Corneal epithelium (CE) covering AM stroma integrated into corneal stroma (pattern 3). (**A**) Semithin microphotograph of CE over corneal stroma (CS) (patient 4, 12 weeks after AMT; original magnification, ×400). Some basal corneal epithelial cells have light cytoplasm, but the superficial epithelial layers are regular. (**B**) TEM of the basal corneal epithelial cells showing signs of degeneration. Cell membranes of basal cells are still connected to each other with desmosomes (*open arrowheads*). (**C**) Hemidesmosomes (*arrow*) are present in low-density patches of basement membrane. (**D**) Corneal epithelium covering AM stroma integrated into corneal stroma of patient 13 (14 weeks after AMT). Semithin microphotograph (original magnification, ×400). Corneal stromal (CS) surface and thickness and number of layers of corneal epithelium (CE) are irregular. The normal structure of the cornea is preserved in the posterior layers. The stromal lesion is not filled but is covered with corneal epithelium. Neither AM epithelium nor AM stroma was identifiable with light microscopy. (**E**) TEM of irregular basal corneal epithelial cells. In the interface between corneal epithelial cells some fibrillar structures, different from those of corneal stroma, and some vacuoli were found, but there was no evidence of persistent AM structure apart from cellular debris (patient 13). (**F**) Higher magnification TEM of the irregular basal corneal epithelial cell (patient 13). Some remnants of the hemidesmosomes (*arrows*) attached them to the underlying corneal stroma. Note the vesiculae (V) and cell debris.

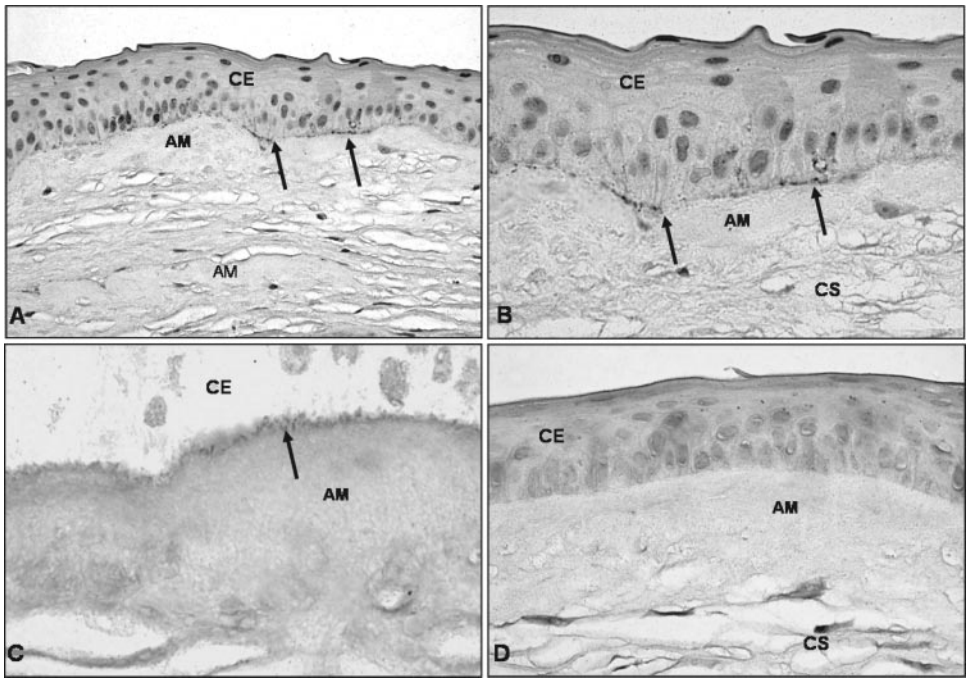

FIGURE 6. Immunohistochemistry of integrin β4 (**A**, **B**), collagen type VII (**C**), and negative control (**D**) in patient 6 (6 weeks after AMT). CS, corneal stroma. (**A**, **B**) Integrin β4: linear immunoreaction along the basal aspect of the corneal epithelium (CE) overgrowing amniotic stroma (AM), indicating the presence of hemidesmosomes (*arrows*; original magnifications: ×200, **A**; ×400, **B**). (**C**) Collagen type VII. Linear fuzzy immunoreaction (*arrow*) along the basal aspect of the corneal epithelium (CE) overgrowing the AM, indicating the presence of anchoring fibrils (original magnification, ×800). (**D**) Negative control using PBS instead of the primary antibody (original magnification, ×400).

density of hemidesmosomes in corneal epithelial cells cultivated on AM and concluded that the adhesion of cultivated corneal epithelial cells to the AM was weaker than in control corneas. In contrast, human corneal epithelial sheets cultivated on AM are described as having adhesion structure properties[35] similar to those of normal corneas. TEM showed that the basal cell layers were well joined to the AM substrate with hemidesmosome attachments. Our findings were similar to those of Nakamura et al.[35]: hemidesmosomes were well developed and were present at a density statistically not lower than that of control corneas. In addition, we did not find any significant difference in desmosome density between control corneal epithelium and corneal epithelium in corneas after AMT.

A novel finding was described in pattern 2—corneal epithelial cells can have hemidesmosomal connection not only on their basal but on their apical surfaces. This happened when corneal epithelium was "sandwiched" by Bowman's layer and AM. The presence of hemidesmosomes on both sides of a corneal epithelial cell suggested that AM stroma provides a suitable surface for corneal epithelial cells to attach to, even in an abnormal orientation. The presence of corneal epithelial cells between AM and Bowman's layer might have been a result of the surgical technical (incomplete abrasion of corneal epithelium before AMT), or perhaps some corneal epithelial cells were able to grow into the AM–Bowman's layer interface from the edge of AM. Histologic and TEM examination did not provide sufficient data to determine unequivocally the origin of these corneal epithelial cells.

The composition of the basement membrane also plays a role in the adhesion of corneal epithelial cells to the underlying matrix. In our specimens the basement membrane was discontinuous, completely missing, or present only in fragments. Some differences were observed in the biomechanical stability of AM after different conservation methods.[36] Stoiber[24] described islands of newly formed collagens in the corneal epithelium–AM interface. Immunohistochemical analysis of the basement membrane of the limbal and AM epithelium was performed by Dietrich et al. (*IOVS* 2005;46:ARVO E-Abstract 2093). The basement membrane composition of AM largely resembled that of the corneal limbal epithelium. The main component of amniotic and corneal basement membrane is type IV collagen. Manifestation of type IV collagen subchains is different in AM, cornea, and conjunctiva. Endo et al.[37] found that cornea and AM manifest primarily in the α5 subchain, whereas Fukuda[38] concluded that AM contained the α2 subchain, which is characteristic of the conjunctiva.

We must consider that the regenerating corneal epithelium in our patients originated from limbal regions with ocular abnormalities, perhaps explaining the decreased volume of basement membrane production. It is suggested that the formation of adhesion structures in corneas after AMT depended on the microenvironment provided by the AM layer(s) and on the capacity of corneal epithelial cells to form hemidesmosomes. Hemidesmosome density seemed to have been regenerated to an extent sufficient to provide the integration of AM stroma for up to 77 weeks after AMT.

We conclude that transplanted AM can integrate into host corneal tissue. During integration, corneal epithelial cells are attached to the AM stroma by hemidesmosomes and basement membrane and are connected to each other by desmosomes. The regeneration of cell–cell and cell–matrix adhesion structures in the corneal epithelium after AMT explains the cellular aspects of AM adhesion to the cornea. However, no adhesion structures between stromal acellular components were identified by TEM; this area remains to be clarified.

References

1. Azuara-Blanco A, Pillai CT, Dua HS. Amniotic membrane transplantation for ocular surface reconstruction. *Br J Ophthalmol*. 1999; 83:399–402.
2. Hanada K, Shimazaki J, Shimmura S, Tsubota K. Multilayered amniotic membrane transplantation for severe ulceration of the corneal and sclera. *Am J Ophthalmol*. 2001;131:324–331.
3. Tseng SCG, Prabhasawat P, Barton K, Gray T, Meller D. Amniotic membrane transplantation with or without limbal allografts for corneal surface reconstruction in patients with limbal stem cell deficiency. *Arch Ophthalmol*. 1998;116:431–441.
4. van Herendael BJ, Oberti C, Brosens I. Microanatomy of the human amniotic membranes: a light microscopic, transmission, and scanning electron microscopic study. *Am J Obstet Gynecol*. 1978;131: 872–880.
5. von Versen-Hoynck F, Syring C, Bachmann S, Moller DE. The influence of different preservation and sterilisation steps on the

histological properties of amnion allografts—light and scanning electron microscopic studies. *Cell Tissue Bank*. 2004;5:45–56.
6. Kruse FE, Rohrschneider K, Volcker HE. Techniques for reconstruction of the corneal surface by transplantation of preserved human amniotic membrane [in German]. *Ophthalmologe*. 1999; 96:673–678.
7. Kruse FE, Meller D. Amniotic membrane transplantation for reconstruction of the ocular surface [in German]. *Ophthalmologe*. 2001; 98:801–810.
8. Dua HS, Azuara-Blanco A. Amniotic membrane transplantation. *Br J Ophthalmol*. 1999;83:748–752.
9. Kim JS, Kim JC, Na BK, et al. Amniotic membrane patching promotes healing and inhibits proteinase activity on wound healing following acute corneal alkali burn. *Exp Eye Res*. 2000;70:329–337.
10. Solomon A, Rosenblatt M, Monroy D, et al. Suppression of interleukin 1alpha and interleukin 1beta in human limbal epithelial cells cultured on the amniotic membrane stromal matrix. *Br J Ophthalmol*. 2001;85:444–449.
11. Park WC, Tseng SCG. Modulation of acute inflammation and keratocyte death by suturing, blood, and amniotic membrane in PRK. *Invest Ophthalmol Vis Sci*. 2000;41:2906–2914.
12. Tseng SC, Li DQ, Ma X. Suppression of transforming growth factor-beta isoforms, TGF-beta receptor type II, and myofibroblast differentiation in cultured human corneal and limbal fibroblasts by amniotic membrane matrix. *J Cell Physiol*. 1999;179:325–335.
13. Talmi YP, Sigler L, Inge E. Antibacterial properties of human amniotic membranes. *Placenta*. 1991;12:285–288.
14. Hao Y, Ma DH, Hwang DG, Kim WS, Zhang F. Identification of antiangiogenic and antiinflammatory proteins in human amniotic membrane. *Cornea*. 2000;19:348–352.
15. Grueterich M, Espana EM, Tseng SC. Ex vivo expansion of limbal epithelial stem cells: amniotic membrane serving as a stem cell niche. *Surv Ophthalmol*. 2003;48:631–646.
16. Ti SE, Grueterich M, Espana EM, Touhami A, Anderson DF, Tseng SCG. Correlation of long term phenotypic and clinical outcomes following limbal epithelial transplantation cultivated on amniotic membrane in rabbits. *Br J Ophthalmol*. 2004;88:422–427.
17. Koizumi N, Fullwood NJ, Bairaktaris G, Inatomi T, Kinoshita S, Quantock AJ. Cultivation of corneal epithelial cells on intact and denuded human amniotic membrane. *Invest Ophthalmol Vis Sci*. 2000;41:2506–2513.
18. Meller D, Pires RT, Tseng SC. Ex vivo preservation and expansion of human limbal epithelial stem cells on amniotic membrane cultures. *Br J Ophthalmol*. 2002;86:463–471.
19. Espana EM, He H, Kawakita T, et al. Human keratocytes cultured on amniotic membrane stroma preserve morphology and express keratocan. *Invest Ophthalmol Vis Sci*. 2003;44:5136–5141.
20. Kruse FE, Rohrschneider K, Völcker HE. Multilayer amniotic membrane transplantation for reconstruction of deep corneal ulcers. *Ophthalmology*. 1999;106:1504–1511.
21. Ferreira De Souza R, Hofmann-Rummelt C, Kruse FE, Seitz B. Multilayer amniotic membrane transplantation for corneal ulcers not treatable by conventional therapy—a prospective study of the status of cornea and graft during follow-up [in German]. *Klin Monatsbl Augenheilkd*. 2001;218:528–534.
22. Kruse FE, Joussen AM, Rohrschneider K, et al. Cryopreserved human amniotic membrane for ocular surface reconstruction. *Graefe's Arch Clin Exp Ophthalmol*. 2000;238:68–75.
23. Gris O, Wolley-Dod C, Güell JL, et al. Histologic findings after amniotic membrane graft in the human cornea. *Ophthalmology*. 2002;109:508–512.
24. Stoiber J, Muss WH, Pohla-Gubo G, Ruckhofer J, Grabner G. Histopathology of human corneas after amniotic membrane and limbal stem cell transplantation for severe chemical burn. *Cornea*. 2002;21:482–489.
25. Seitz B, Resch M, Schlötzer-Schrehardt U, Hofmann-Rummelt C, Sauer R, Kruse FE. Histology and ultrastructure of corneas after amniotic membrane transplantation. *Arch Ophthalmol*. In press.
26. Seitz B, Ferreira de Souza R, Hofmann-Rummelt C, et al. Patch, graft or sandwich for persistent corneal ulcers—differentiated technique of amniotic membrane transplantation (Abstract). *Clin Exp Ophthalmol*. 2002;30:122.
27. Prabhasawat P, Tesavibul N, Komolsuradej W. Single and multilayer amniotic membrane transplantation for persistent corneal epithelial defect with and without stromal thinning and perforation. *Br J Ophthalmol*. 2001;85:1455–1463.
28. Letko E, Stechschulte SU, Kenyon KR, et al. Amniotic membrane inlay and overlay grafting for corneal epithelial defects and stromal ulcers. *Arch Ophthalmol*. 2001;119:659–663.
29. Küchle M, Seitz B, Langenbucher A, Naumann GO. Nonmechanical excimer laser penetrating keratoplasty for perforated or predescemetal corneal ulcers. *Ophthalmology*. 1999;106:2203–2209.
30. Seitz B, Langenbucher A, Nguyen NX, Kus MM, Kuchle M, Naumann GO. Results of the first 1,000 consecutive elective nonmechanical keratoplasties using the excimer laser: a prospective study over more than 12 years [in German]. *Ophthalmologe*. 2004;101:478–488.
31. Seitz B, Langenbucher A, Kuchle M, Naumann GO. Impact of graft diameter on corneal power and the regularity of postkeratoplasty astigmatism before and after suture removal. *Ophthalmology*. 2003;110:2162–2167.
32. Connon CJ, Nakamura T, Quantock AJ, Kinoshita S. The persistence of transplanted amniotic membrane in corneal stroma. *Am J Ophthalmol*. 2006;141:190–192.
33. Tosi GM, Traversi C, Schuerfeld K, et al. Amniotic membrane graft: histopathological findings in five cases. *J Cell Physiol*. 2005;202: 852–857.
34. Madigan MC, Holden BA. Reduced epithelial adhesion after extended contact lens wear correlates with reduced hemidesmosome density in cat cornea. *Invest Ophthalmol Vis Sci*. 1992;33: 314–323.
35. Nakamura T, Yoshitani M, Rigby H, et al. Sterilized, freeze-dried amniotic membrane: a useful substrate for ocular surface reconstruction. *Invest Ophthalmol Vis Sci*. 2004;45:93–99.
36. Adds PJ, Hunt CJ, Dart JKG. Amniotic membrane grafts, "fresh " or frozen? a clinical and in vitro comparison. *Br J Ophthalmol*. 2001;85:905–907.
37. Endo K, Nakamura T, Kawasaki S, Kinoshita S. Human amniotic membrane, like corneal epithelial basement membrane, manifests the alpha5 chain of type IV collagen. *Invest Ophthalmol Vis Sci*. 2004;45:1771–1774.
38. Fukuda K, Chikama T, Nakamura M, Nishida T. Differential distribution of subchains of the basement membrane components type IV collagen and laminin among the amniotic membrane, cornea, and conjunctiva. *Cornea*. 1999;18:73–79.